



Cite this: *Mater. Chem. Front.*,  
2024, 8, 800

## Defect passivation engineering of wide-bandgap perovskites for high-performance solar cells

Xiao Wu,<sup>†,a</sup> Guoqing Xiong,<sup>†,a</sup> Ziyao Yue,<sup>a</sup> Ziyao Dong<sup>b</sup> and Yuanhang Cheng <sup>id, \*</sup>

Wide-bandgap (WBG) mixed-halide perovskite solar cells (PVSCs) exhibit a wide range of applicability, such as tandem photovoltaics (PVs), underwater PVs, space PVs, and building-integrated photovoltaics (BIPVs). However, the state-of-the-art WBG mixed-halide PVSCs still suffer from phase segregation and large open-circuit voltage ( $V_{oc}$ ) loss, which significantly limit the overall power conversion efficiency of devices. A dominant source of these limitations is the presence of defects within the mixed-halide perovskite lattice structure and at interfaces between the perovskite and carrier transport layers (CTLs). In response, various device engineering strategies have been implemented to passivate the defects and improve device performance. Therefore, in this comprehensive review, different types of defects inherent in WBG mixed-halide perovskites were firstly described, followed by their detrimental effects on perovskite materials and corresponding device performance. Furthermore, several device engineering strategies to passivate the defects at perovskite buried interface, perovskite bulk, and perovskite surface had been summarized, respectively. These defect passivation schemes provided a forward-oriented perspective on forthcoming strategies for WBG mixed-halide PVSCs. These strategies not only offered valuable guidance for realizing enhanced efficiency but also improved the phase stability of WBG mixed-halide PVSCs in the pursuit of high-performance PV technology.

Received 31st August 2023,  
Accepted 10th November 2023

DOI: 10.1039/d3qm00970j

rsc.li/frontiers-materials

<sup>a</sup> School of New Energy, Nanjing University of Science and Technology, Jiangyin, Jiangsu 214443, China. E-mail: yhcheng@njust.edu.cn

<sup>b</sup> School of Energy and Environment, Anhui University of Technology, Maanshan, Anhui 243002, China

† These authors contributed equally.



Xiao Wu

*Wu Xiao is a final year student at the School of New Energy at Nanjing University of Science and Technology (NJUST). Currently, she is working on a final year project under the supervision of Prof. Yuanhang Cheng at NJUST. Her current research focuses on highly efficient perovskite photovoltaic device fabrication and characterization.*



Yuanhang Cheng

*Yuanhang Cheng is a professor at the School of New Energy of Nanjing University of Science and Technology (NJUST). Before joining NJUST, he worked as a research associate at the City University of Hong Kong (CityU) from 2021 to 2022. He was a research fellow at the Solar Energy Research Institute of Singapore (SERIS), National University of Singapore (NUS) from 2018 to 2021. He completed his PhD from CityU in October 2017 under the guidance of Prof. Stephen Sai-Wing Tsang. His research interests include perovskite solar cells, highly efficient perovskite/Si tandem solar cells, new photovoltaic materials with various organic-inorganic composites, and solar-powered photoelectrochemical applications.*

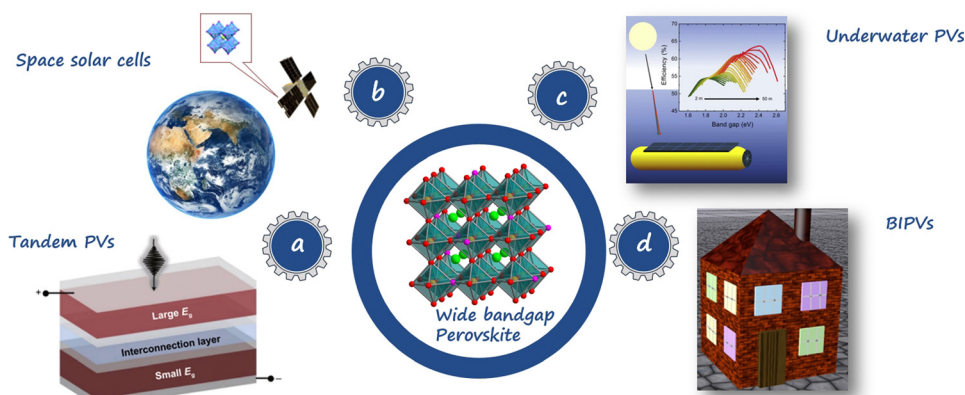


Fig. 1 Various applications of WBG mixed-halide PVSCs, including (a) space PVs, (b) tandem PVs, (c) underwater PVs, and (d) BIPVs. Reproduced with permission from ref. 33. Copyright 2021, Springer Nature. Reproduced with permission from ref. 34. Copyright 2020, Elsevier.

deleterious. Therefore, in pursuit of sustainable and ecologically harmonious living, resorting to renewable energy sources, especially solar energy, has gained paramount significance.<sup>2,3</sup> This shift has led to the prominence of solar cells, pivotal technologies capable of converting photons into electrons through the photovoltaic (PV) effect, heralding an era of enduring and ecologically conscious progress.<sup>4–7</sup> Within the PV community, beyond the Si-based solar cells and thin-film solar cells that have been successfully commercialized, perovskite solar cells (PVSCs) have been unequivocally regarded as the most promising devices throughout the past decade. This distinction is attributed to their outstanding optoelectronic characteristics,<sup>8–10</sup> simple low-temperature solution processing,<sup>11–13</sup> and low-cost fabrication methods.<sup>14–16</sup>

Perovskites represent a class of materials characterized by the  $ABX_3$  crystal structure. In metal halide perovskites, the A-site can be occupied by  $\text{CH}_3\text{NH}_3^+$  ( $\text{MA}^+$ ),  $\text{HC}(\text{NH}_2)_2^+$  ( $\text{FA}^+$ ), or  $\text{Cs}^+$ , while the B-site is typically filled with  $\text{Pb}^{2+}$  or  $\text{Sn}^{2+}$ , and X denotes halide anions such as  $\text{I}^-$ ,  $\text{Br}^-$ , and  $\text{Cl}^-$ .<sup>17</sup> The perovskite materials,  $\text{CH}_3\text{NH}_3\text{PbI}_3$  and  $\text{CH}_3\text{NH}_3\text{PbBr}_3$ , were firstly introduced as solar absorbers in dye-sensitized solar cells (DSSCs) in 2009.<sup>18</sup> However, the liquid-based electrolytes within DSSC systems result in their rapid degradation. The turning point came in 2012 with the introduction of solid-state hole transport layer (HTL), facilitating the rapid and unprecedented development of PVSCs in the last decade.<sup>19</sup> To date, the certified power conversion efficiency (PCE) of perovskite-based single junction solar cells has reached 26.1%,<sup>20</sup> approaching that of Si-based solar cells. This could be attributed to outstanding optoelectronic characteristics of the organic-inorganic metal halide perovskites, including high absorption coefficients,<sup>21</sup> long carrier diffusion lengths,<sup>22</sup> long carrier lifetime,<sup>23</sup> low recombination rates,<sup>24</sup> and high defect tolerance.<sup>25</sup> Moreover, the bandgaps of perovskites can be tuned by simply changing the composition,<sup>26</sup> expanding their applications wider than any other PV technologies. Especially for organic-inorganic mixed-halide perovskites with a bandgap greater than 1.65 eV, which are referred to as wide-bandgap (WBG) perovskites, exhibit even more tremendous potential in various PV applications.<sup>27</sup>

As shown in Fig. 1a, the WBG perovskites can be employed as top cells in perovskite/silicon and perovskite/perovskite tandem PVs, which can surpass the efficiency limit of single-junction solar cell (33%), pushing the theoretical PCE towards a value of 46%.<sup>28,29</sup> As materials with bandgaps over 1.8 eV hold the potential for absorbing blue-to-yellow light, the WBG PVSCs can also be applied to underwater PVs,<sup>30</sup> as shown in Fig. 1b. Fig. 1c shows that WBG PVSCs can serve as important candidate technologies for space solar cells,<sup>31</sup> which have apparent tolerance to high-energy proton radiation. Moreover, the colorful appearance and flexibility of WBG PVSCs make them promising candidates for building-integrated photovoltaics (BIPVs) (Fig. 1d).<sup>32</sup> The WBG perovskites not only exhibit excellent response to outdoor and indoor lighting but offer additional aesthetic advantages due to their semi-transparency and various color choices.

It has been demonstrated that the bandgap of metal halide perovskites primarily depends on the coupling between the B-site cation and the X-site anion.<sup>35</sup> Reducing the lattice size of perovskites will increase the wavefunction overlap and thus result in a wider bandgap. Therefore, the WBG perovskites are generally obtained by replacing the iodine (I) ions with bromine (Br) ions.<sup>27,36</sup> However, the state-of-the-art WBG mixed-halide PVSCs still suffer from issues of large open-circuit voltage ( $V_{oc}$ ) loss and phase segregation.<sup>27,37</sup> Such issues limit the performance and applications of WBG perovskites, and the phase segregation caused by the migration of I and Br ions exacerbates the instability issue under illumination, making the degradation of WBG mixed-halide PVSCs even more rapid.<sup>38,39</sup> A comprehensive understanding of the mechanisms behind these issues remains limited; however, the unavoidable generation of various defects during PVSCs fabrication processes is generally considered as one of the primary factors.<sup>27,40</sup> On the one hand, defects act as non-radiative recombination centers, reducing the PCE of devices.<sup>41</sup> On the other hand, defects act as transport channels for migration of ions, facilitating the phase segregation and causing the degradation of PVSCs.<sup>9,42</sup>

Both phase segregation and defects can contribute to instability in WBG perovskites.<sup>43</sup> On the one hand, the migration of

halide anions, facilitated by structural defects within the perovskite lattice, exerts a significant influence on phase segregation. Investigations have indicated that phase segregation predominantly manifests at grain boundaries, known for their heightened defect density compared to the grain interior.<sup>44</sup> Therefore, it is suggested that defects are involved in initiating the phase segregation process.<sup>45</sup> On the other hand, phase segregation will induce more defects in the perovskite lattice structure due to the migration of the ions. The emergence of these new defects accelerates the deterioration of device performance, thereby contributing to the instability of WBG mixed-halide perovskites.<sup>46</sup> Nevertheless, the precise governing factor between phase segregation and defects in the context of WBG perovskite instability remains a topic of ongoing debate in the scientific community.

Despite that the whole picture of these issues is still uncovored, addressing the relevant part of defects can contribute to overall improvement of device performance. As a result, numerous defect passivation methods have been reported for achieving high-performance WBG mixed-halide PVSCs.<sup>47–58</sup> Therefore, in this review, we firstly described different types of defects in WBG mixed-halide perovskites. Then, the impact of defects on the performances of both perovskite materials and devices has been discussed. Subsequently, passivation criteria along with strategies to passivate different types of defects are summarized, respectively. Finally, a forward-looking perspective on future passivation strategies for mixed-halide WBG PVSCs was provided, offering valuable guidance for the development of high-efficiency and phase-stable WBG mixed-halide PVSCs.

## 2 Defects in mixed-halide perovskites

The defects, namely the incomplete ion coordination within the perovskite materials, can form electron trap states within the bandgap, inducing the  $V_{oc}$  loss and correspondingly lower PCEs.<sup>59</sup> Defects primarily occur at perovskite interfaces and grain boundaries.<sup>27,60</sup> Taking  $\text{MAPbI}_3$  as an example, the common defects include vacancy defects ( $\text{V}_{\text{MA}}$ ,  $\text{V}_{\text{Pb}}$ , and  $\text{V}_{\text{I}}$ ), interstitial defects ( $\text{MA}_{\text{i}}$ ,  $\text{Pb}_{\text{i}}$ , and  $\text{I}_{\text{i}}$ ), and antisite defects ( $\text{MA}_{\text{Pb}}$ ,  $\text{MA}_{\text{I}}$ ,  $\text{Pb}_{\text{MA}}$ ,  $\text{Pb}_{\text{I}}$ ,  $\text{I}_{\text{MA}}$ , and  $\text{I}_{\text{Pb}}$ ).<sup>61</sup>

In WBG perovskite materials, such as  $\text{MAPbBr}_3$  or  $\text{MAPbI}_{3-x}\text{Br}_x$ , both vacancies, interstitials, and antisite defects are also included. (1) For the vacancies, these defects occur when a lattice site within the crystal structure is unoccupied by an atom or ion. In WBG perovskites, vacancies can involve either the organic cation (e.g.,  $\text{V}_{\text{MA}}$ ) or the halide anion (e.g.,  $\text{V}_{\text{I}}$ ). These vacancies lead to the presence of uncoordinated lead or halogen ions within the crystal lattice.<sup>62</sup> (2) For the interstitial defects, the interstitials refer to atoms or ions that occupy positions between the normal lattice sites. For WBG perovskites, interstitials can involve excess lead (e.g.,  $\text{Pb}_{\text{i}}$ ), excess halogen (e.g.,  $\text{I}_{\text{i}}$  or  $\text{Br}_{\text{i}}$ ), or excess organic cations (e.g.,  $\text{MA}_{\text{i}}$ ) which disrupt the regular arrangement of atoms and introduce additional defect states.<sup>63</sup> (3) For the antisite defects, they specifically arise when different types of atoms or ions

exchange positions within the crystal lattice. In WBG perovskites, this can occur between the organic cations, lead cations and halide anions, such as  $\text{MA}_{\text{I}}$ ,  $\text{MA}_{\text{Br}}$ ,  $\text{I}_{\text{Pb}}$ ,  $\text{Br}_{\text{Pb}}$  and so on.<sup>64–66</sup> Antisite defects can introduce energy levels within the bandgap, leading to trap states that degrade device performance.<sup>66</sup>

Owing to the ionic property of perovskite materials, as shown in Fig. 2a, defects are generally positively or negatively charged.<sup>67</sup> The charged defects act as “traps” that can capture charge carriers of opposite polarity and thus induce non-radiative recombination, causing  $V_{oc}$  loss and low PCEs in PV devices. Normally, the formation energies of vacancy defects are lower than those of interstitial defects, and the antisite defects have the highest formation energy.<sup>58,64,68–70</sup> On the other hand, vacancy defects generally exhibit shallow energy levels, while most of interstitial and antisite defects are considered as deep-level defects that trigger the notorious non-radiative recombination in solar cells.<sup>71–73</sup> For example, Z. Ni, *et al.* have elucidated that the negative ( $\text{I}_{\text{i}}^-$ ) or positive ( $\text{I}_{\text{i}}^+$ ) halide interstitials are the two main deep-level defects in the pure I-based perovskites.<sup>74</sup>

In WBG mixed-halide perovskites, such as  $\text{MAPb}(\text{I}_{1-x}\text{Br}_x)_3$ , it has been reported that phase segregation is more likely to occur when the bromide content falls in the range of  $0.2 < x < 0.8$  (Fig. 2a).<sup>27</sup> Therefore, under such conditions, both phase segregation and defects play important roles in influencing the stability of perovskite materials and devices. However, under the condition with the bromide content lower than 20% or higher than 80%, the phase segregation is suppressed, and the defects may play a dominant role in determining the performance of perovskite devices. It is important to exclude the impact of phase segregation to identify the nature of the trap defects, as the phase segregation will make the defects types and densities more dynamic and more difficult to capture. Yang *et al.* have measured both the trap density of states (tDOS) and their energetic distribution in  $\text{Cs}_{0.1}\text{FA}_{0.2}\text{MA}_{0.7}\text{Pb}(\text{I}_{1-x}\text{Br}_x)_3$  ( $x < 0.2$ ) through thermal admittance spectroscopy (TAS).<sup>64</sup> As shown in Fig. 2b, the two similar trap bands centered at  $\sim 0.12$  eV and  $\sim 0.35$  eV in  $\text{Cs}_{0.1}\text{FA}_{0.2}\text{MA}_{0.7}\text{PbI}_3$  and  $\text{Cs}_{0.1}\text{FA}_{0.2}\text{MA}_{0.7}\text{Pb}(\text{I}_{0.85}\text{Br}_{0.15})_3$  indicated that the Br incorporation did not introduce new types of charge traps. However, as shown in Fig. 2c, with the Br percentage increasing from 0 to 20%, tDOS considerably increased in the deep trap region (0.3–0.4 eV). Through measuring the tDOS of  $\text{Cs}_{0.1}\text{FA}_{0.2}\text{MA}_{0.7}\text{PbI}_3$  and  $\text{Cs}_{0.1}\text{FA}_{0.2}\text{MA}_{0.7}\text{Pb}(\text{I}_{0.85}\text{Br}_{0.15})_3$  in an I-rich environment (Fig. 2d) and Br-rich environment (Fig. 2e), they found that the main deep charge traps are still I interstitials, similar in the pure I-based perovskites. To further identify whether the main defects are negative ( $\text{I}_{\text{i}}^-$ ) or positive ( $\text{I}_{\text{i}}^+$ ) halide interstitials, they also found that the deep traps will move towards the poly[bis(4-phenyl)(2,4,6-trimethylphenyl)amine] (PTAA) side, as depicted in Fig. 2f and g, indicating they are positively charged. However, this study did not furnish details concerning other defects present in the WBG perovskite, and the impact of phase segregation (when  $x > 0.2$ ) on the defects formation was also not described. Although more works on the nature and properties of defects in WBG perovskites are required to elucidate

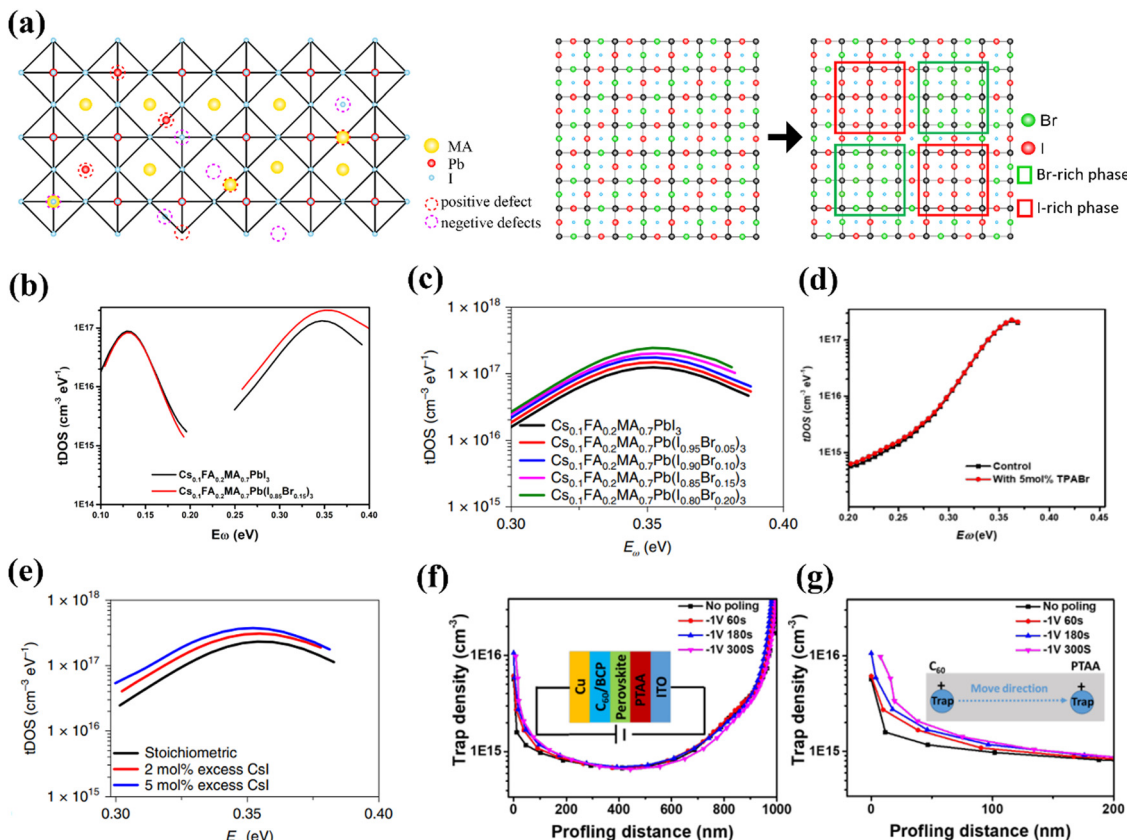


Fig. 2 (a) Various positively or negatively charged defects present in  $\text{MAPbI}_3$  and phase separation in WBG perovskites. (b) tDOS spectra of  $\text{Cs}_{0.1}\text{FA}_{0.2}\text{MA}_{0.7}\text{PbI}_3$  and  $\text{Cs}_{0.1}\text{FA}_{0.2}\text{MA}_{0.7}\text{Pb}(\text{I}_{0.85}\text{Br}_{0.15})_3$  determined from temperature dependent capacitance-frequency measurement. (c) tDOS spectra of  $\text{Cs}_{0.1}\text{FA}_{0.2}\text{MA}_{0.7}\text{Pb}(\text{I}_{1-x}\text{Br}_x)_3$  ( $x = 0, 5\%, 10\%, 15\%$  and  $20\%$ ) solar cells. (d) tDOS spectra of WBG devices with and without trimethylphenylammonium bromide (TPABr). (e) tDOS spectra of  $\text{Cs}_{0.1}\text{FA}_{0.2}\text{MA}_{0.7}\text{Pb}(\text{I}_{0.85}\text{Br}_{0.15})_3$  solar cells with and without excess CsI. (f) Trap density of  $\text{Cs}_{0.1}\text{FA}_{0.2}\text{MA}_{0.7}\text{Pb}(\text{I}_{0.85}\text{Br}_{0.15})_3$  perovskite solar cells before and after applying the reverse bias measurement (DLCP). (g) The magnified plots near the  $\text{C}_{60}$ /perovskite interface in (f). Reproduced with permission from ref. 64. Copyright 2022, Springer Nature.

their impacts on device performance, it is known that the defects are traps for charge carriers and they also serve as active sites for water and oxygen erosion, accelerating the degradation of perovskites.<sup>27</sup>

### 3 Passivators for defects

Passivation refers to the process of reducing defects and improving the surface properties of the perovskite materials, thereby enhancing its device performances and operational stability. Since WBG mixed-halide perovskites often suffer from severe  $V_{oc}$  loss and instability issue due to their high defect densities, eliminating these defects is often of great significance to achieve better performance of the devices.

General criteria for passivation is determined by the charged nature of these defects. For instance, in the case of positively charged defects caused by under-coordinated  $\text{Pb}^{2+}$  ions, such as vacancies, Lewis bases containing atoms capable of providing lone pairs of electrons (e.g., O, S, N, and P) can passivate them through coordination bonding.<sup>75,76</sup> Alternatively, anions like iodide, bromide, and thiocyanate can passivate these defects

through ionic bonding.<sup>77-79</sup> The passivation of negatively charged defects resulting from excess electrons associated with under-coordinated I ions or I-Pb antisite defects can be achieved using Lewis acids capable of accepting pairs (e.g. fullerene) or structures containing abundant highly electronegative elements like F, which enable partial structures suitable for accepting electron pairs.<sup>80-82</sup> Passivation can also occur through hydrogen bonding between iodide ions and hydrogen atoms attached to highly electronegative elements like O or N, or through ionic bonding with ammonium cations or metal cations.<sup>83,84</sup>

It is worth noting that from the aspect of passivating the defects, there is not much difference in defect passivation strategies between WBG and narrow-bandgap PVSCs. This is because WBG materials, such as  $\text{MAPbBr}_3$  or  $\text{MAPbI}_{3-x}\text{Br}_x$ , exhibit a similar composition of defect chemistry compared to their narrow-bandgap counterparts like  $\text{MAPbI}_3$ , which has been described in the previous section. These compositions include vacancies (e.g.,  $\text{V}_{\text{MA}}$  or  $\text{V}_{\text{I}}$ ), interstitials (e.g.,  $\text{Pb}_i$  or  $\text{I}_i$ ), and antisite defects (e.g.,  $\text{MA}_i$  or  $\text{I}_{\text{Pb}}$ ). These defects result in uncoordinated lead or halogen ions (such as iodine or bromine ions) in the perovskite lattice structure and thus inducing the degradation of WBG PVSCs.

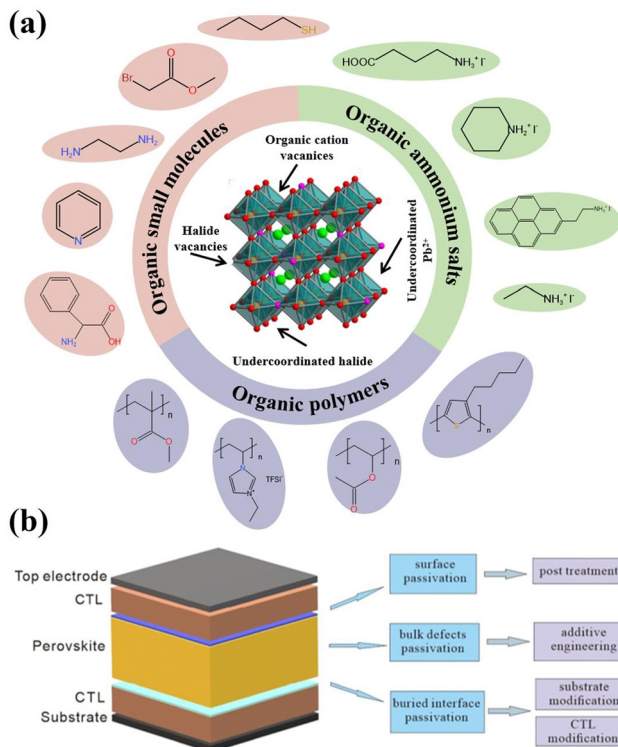


**Fig. 3** (a) Depiction of the passivator molecules for different defects in WBG perovskites (b) three categories of passivation methods for WBG PVSCs

As shown in Fig. 3a, to passivate the uncoordinated lead ions in both wide bandgap or the narrow bandgap perovskites, some Lewis bases, alkali metal halides, crown ethers, small molecules, or polymers containing carboxylic acid or phosphoric acid groups can be used. For passivating the uncoordinated halide ions (bromide or iodide), Lewis acids, small molecules, or polymers containing amino or sulfonic acid groups can be employed. Additionally, during the fabrication process, different materials and strategies can be applied to eliminate defects at different positions in the PVSCs. As shown in Fig. 3b, the passivation strategies can also be divided into 3 categories, including the buried-interface defect passivation, the bulk defect passivation, and the surface defect passivation, which can be classified by the deposition of perovskites. The passivation method applied prior to perovskite deposition is denoted as “buried interface passivation”, which aims to mitigate the defects at the interface of perovskite and CTL. The term “bulk defects passivation” refers to the concurrent execution of the passivation method and perovskite deposition, with the objective of reducing the bulk defects within the perovskite films. The post-implementation of the passivation method is specifically designed to minimize the perovskite surface defects, termed “surface defects passivation”.

To efficiently passivate the defects, it is important to select suitable strategies and corresponding passivators. For the WBG perovskites, another tough issue is the phase segregation of perovskites under illumination. Therefore, strategies to

passivate defects and suppress the phase segregation at the same time for WBG perovskites were also introduced. In this section, we summarized the passivation methods have been proposed by researchers for WBG PVSCs so far and divided them into three categories, including buried interface passivation, bulk defects passivation and surface passivation. For each category we also introduced several different passivation strategies for different defect types.

## 4 Device passivation engineering for WBG PVSCs

## 4.1 Buried interface passivation

**4.1.1 Self-assembled monolayers (SAMs) to passivate the buried interface defects.** Buried interface passivation is a technique used to improve the performance and stability of WBG PVSCs *via* addressing defects and surface recombination at the interface between perovskite layer and deposited CTL. This approach involves introducing passivating layers or interfacial materials between different functional layers to inhibit non-radiative recombination and enhance charge extraction.<sup>81,85</sup>

Self-assembled monolayers (SAMs) have been investigated as surface passivators in PVSCs to improve the device performance and stability, SAMs are organic molecules that can spontaneously arrange themselves into an ordered monolayer on the substrate, providing a tunable interface between the perovskite layer and the other functional layers within the device.<sup>86,87</sup> The ordered array of organic molecules contains an anchoring group that can bond to the substrate and a functional head-group.<sup>87</sup> The headgroups often have hydrophilic functional groups to tune their surface properties. In addition, headgroups such as ammonium groups ( $-\text{NH}_3$ ) and carboxyl ( $-\text{COOH}$ ) can passivate the defects at the upper perovskite, which will effectively enhance the PV performance of the device.<sup>88</sup> As depicted in Fig. 4a, SAMs play the role of linkers, bonding the substrate and perovskite films tightly to eliminate interfacial voids. Moreover, SAMs are cheap, dopant-free, simple to process and intrinsically scalable compared to normal carrier transport materials (CTMs).<sup>89-91</sup>

It is worth noting that while SAMs offer promising benefits, selecting appropriate molecules carefully, understanding their interactions with the perovskite materials, and optimizing their deposition techniques are crucial for achieving desired improvements in PVSCs. For example, Albrecht *et al.* have proposed new types of SAMs as the hole transport layers (HTL) for perovskite/CIGS tandem solar cells (TSCs).<sup>92</sup> These new SAMs can offer a crucial advantage of conformal coverage on the rough CIGS film surface compared to spiro-OMeTAD and PTAA. In the work, they employed three different SAMs, namely (2-[3,6-bis[bis(4-methoxyphenyl)amino]-9H-carbazol-9-yl]ethyl)phosphonic acid (V1036), MeO-2PACz and [2-(9H-carbazol-9-yl)ethyl]phosphonic acid (2PACz). Fig. 4b illustrates three SAM molecules for PVSCs, among which the 2PACz exhibited the highest efficiency of 20.9% for the  $\text{Cs}_{0.05}(\text{MA}_{0.17}\text{FA}_{0.83})_{0.95}\text{Pb}(\text{I}_{0.83}\text{Br}_{0.17})_3$  solar cells and an efficiency of 23.26%

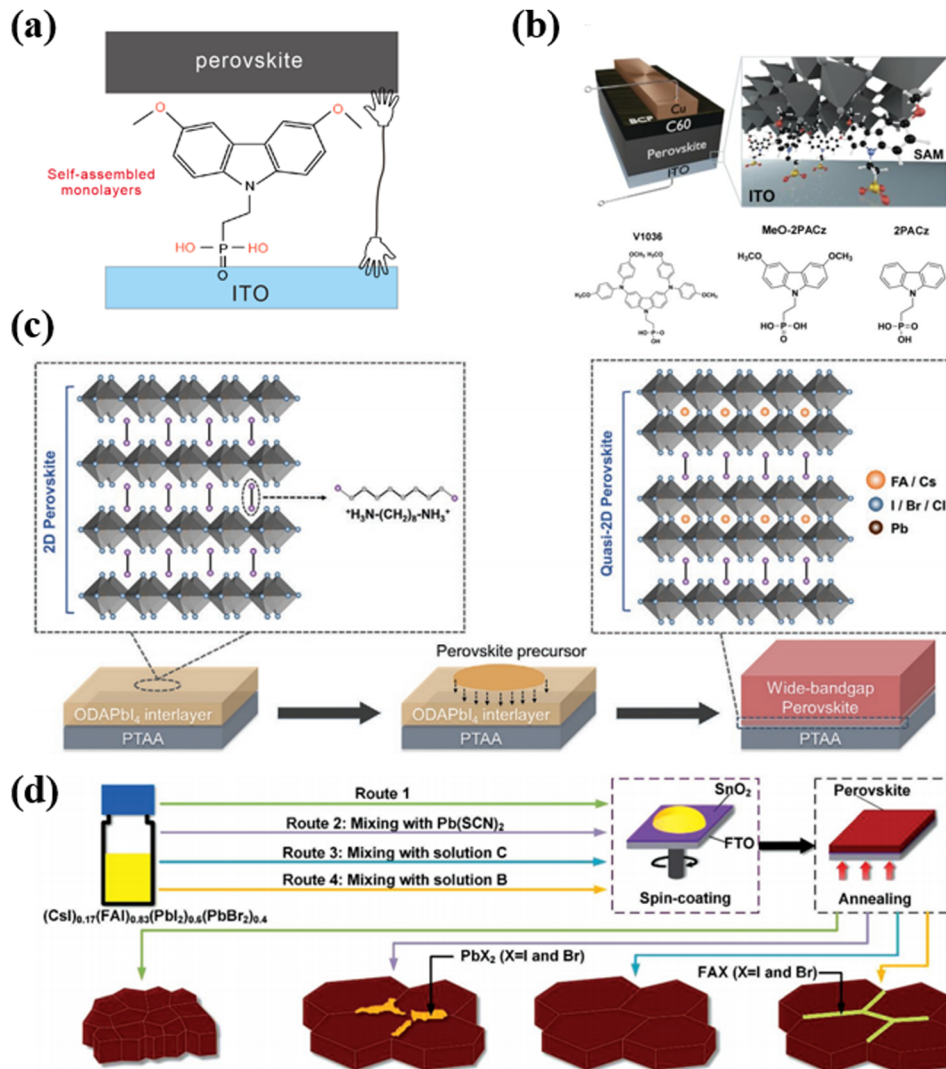


Fig. 4 (a) The working mechanism of SAMs. (b) Schematic of the device structure, visualizing how the SAM molecules attach to the ITO surface and contact the upper perovskite. Reproduced with permission from ref. 89. Copyright 2019, Royal Society of Chemistry. (c) Schematic illustration of constructing the quasi-2D perovskite interface by the ODAPbI<sub>4</sub> interlayer. Reproduced with permission from ref. 53. Copyright 2021, Wiley-VCH. (d) Schematic diagram of spin-coating stoichiometrically mixed precursor solution on the tin dioxide substrate. Reproduced with permission from ref. 49. Copyright 2018, Wiley-VCH.

for perovskite/CIGS TSCs.<sup>93</sup> In addition, the methyl-substituted carbazole monolayer named Me-4PACz ([4-(3,6-dimethyl-9H-carbazol-9-yl)butyl]phosphonicacid) was also used as HTL, which can allow fast hole extraction and minimize non-radiative recombination. Meanwhile, the Me-4PACz substrate can especially improve the photostability of continuous illumination.<sup>93</sup>

**4.1.2 Low-dimensional perovskites to passivate buried interfaces.** Low-dimensional perovskites refer to perovskite materials that have reduced dimensions compared to traditional three-dimensional (3D) perovskites, which show altered crystal structures and unique electronic properties when applied on ITOs before generating traditional 3D perovskites.<sup>94</sup> This passivation technique aims to enable better growth of 3D perovskites with fewer defects, enhancing charge transport, reducing nonradiative recombination, and improving the efficiency and stability of the devices.<sup>95</sup>

In terms of application, different strategies and materials are adopted for corresponding substrates such as PTAA or SnO<sub>2</sub>. As shown in Fig. 4c, Wang *et al.* have developed an ingenious and effective way to achieve high-efficiency WBG PVSCs by adopting a 2D perovskite (ODAPbI<sub>4</sub>) interlayer on the top of PTAA.<sup>53</sup> The long-chain ODA cation could diffuse into the upper WBG perovskite to modulate the crystal growth and reduce the charge trap density of the perovskite during film processing. Simultaneously, the formation of ODA-based quasi-2D perovskite at the hole-selective interface facilitates the effective hole extraction to HTL. These joint effects efficiently inhibited non-radiative recombination loss, improving the PCE of WBG PVSCs ( $E_g \approx 1.66$  eV) to 21.05% with an impressive  $V_{oc}$  of 1.23 V.

For substrate SnO<sub>2</sub>, Zhou *et al.* proposed a way to reduce defects as shown in Fig. 4d.<sup>49</sup> Firstly, the stoichiometrically

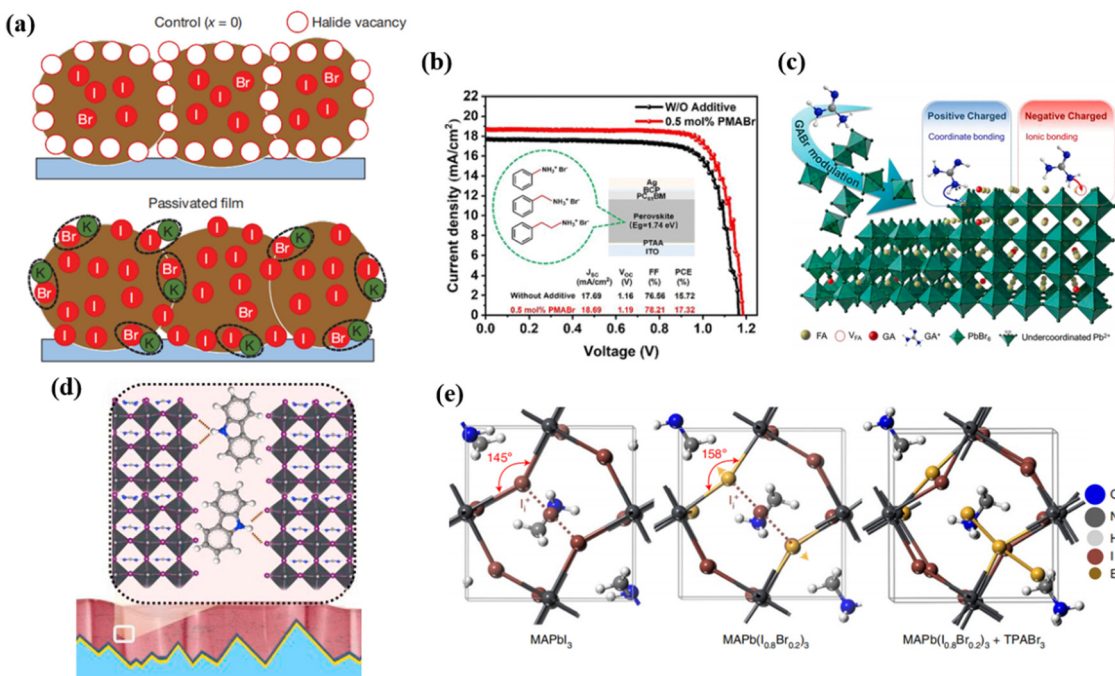


**Fig. 5** (a) Schematic of the passivation mechanism of  $K^+$ , in which the excessive halide is immobilized through complexing with potassium into benign compounds at the grain boundaries. Reproduced with permission from ref. 54. Copyright 2018, Springer Nature. (b)  $J-V$  characteristics of the WB-PSCs with three additives. Reproduced with permission from ref. 56. Copyright 2022, ACS Appl. (c) Schematic mechanism of GABr modulation on  $FAPbBr_3$  based PVSCs. Reproduced with permission from ref. 51. Copyright 2022, Elsevier. (d) Schematic illustration of interaction of carbazole with perovskite films. Reproduced with permission from ref. 47. Copyright 2021, Elsevier. (e) Geometrical structures of  $MAPbI_3$  and  $MAPb(I_{0.8}Br_{0.2})_3$  with iodide interstitials, and the calculated geometrical structure of  $MAPb(I_{0.8}Br_{0.2})_3$  with  $Br_3^-$ . Reproduced with permission from ref. 58. Copyright 2021, Springer Nature.

mixed precursor solution was spin-coated on a hydrophilic  $SnO_2$  surface to get a perovskite thin film with low crystallinity and small grain size. Then the grain crystallization and surface chemistry were modified by selectively adding  $Pb(SCN)_2$ , excess FAX, or a combination of both. The results greatly reflected the improved crystallinity, reduced impurity, and passivated grain boundary.

#### 4.2 Additive engineering to passivate the perovskite bulk

Additive engineering includes incorporating passivating additives to the perovskite precursor solution, and has been widely used to passivate bulk defects within perovskites to improve the stability and efficiency of PVSCs. Additives can act as surfactants or stabilizers, improving the passivation quality and reducing bulk defects.<sup>50,96</sup> The choice of additives depends on their compatibility with the perovskite material and their ability to reduce trap states.<sup>97</sup> Various additives are constantly being discovered for corresponding defects.

Potassium ( $K^+$ ) ion doping has been identified as an effective approach in additive engineering. Abdi-Jalebi *et al.* proposed that the  $K^+$  doping in mixed perovskites can reduce non-radiative recombination loss *via* passivating the grain boundary with potassium halide layers.<sup>54</sup> Based on their viewpoint, the  $K^+$  doping would produce  $KI/KBr$  compounds which mainly distribute at the grain boundary, thus, immobilize the halide ions and vacancies, this can be vividly shown in Fig. 5a. In order to

compensate for any halide vacancies, they introduced excess iodide to the perovskite precursor solutions by using potassium iodide. The excess halides are immobilized in the form of benign, potassium-rich, halide-sequestering species at the grain boundaries, filling these vacancies to passivate the non-radiative recombination, inhibiting halide migration and suppressing additional non-radiative recombination loss caused by interstitial halides.

In addition, long chain ammonium cations were commonly used to passivate grain boundaries of perovskite films. Huo *et al.* reported a way of adding organic bromide salts with different chain lengths involving phenylammonium bromide (PhABr), phenethylammonium bromide (PMABr) and phenethylammonium bromide (PEABr) to the perovskite precursor to passivate the defects in WBG PVSC (1.74 eV), as shown in Fig. 5b.<sup>56</sup> They found that PMABr with moderate chain lengths achieved a PCE of 17.32% with enhanced  $V_{oc}$ , performing the best compared to those of the standard device (15.72%) and the devices with PhABr (15.98%) or PEABr additives (16.83%).

It is widely known to use organic small molecules and polymers with Lewis acid or basic groups to passivate defects at grain boundaries of perovskite. Xu *et al.* added guanidinium bromide (GABr) to the  $FAPbBr_3$  precursor to passivate the charged defects of the perovskite.<sup>51</sup> It was proposed that negatively charged (A-site vacancy) and positively charged (uncoordinated  $Pb^{2+}$ ) defects can be simultaneously passivated

by the ionized  $-\text{NH}_3^+$  group and unsaturated N atoms. As can be seen from Fig. 5c, the amine (and/or imine) group, namely that of a Lewis base, anchored with the under-coordinated  $\text{Pb}^{2+}$  by sharing lone-pair electrons. Conversely, the ammonium cation could passivate negatively charged defects by ionic bonding like A-site vacancy. Thereby, incorporation of  $\text{GA}^+$  simultaneously passivates both positively and negatively charged defects of the perovskite by multi-reactive site anchoring, transforming the perovskite from charge-rich to charge-neutral region. Liu *et al.* introduced carbazole to inhibit phase segregation and heal deep-level charged defects of WBG perovskites.<sup>47</sup> Generally, the ion migration is activated by strain and starts from grain boundaries. As shown in Fig. 5d, through hydrogen bonding interactions with halides, the carbazole molecules can effectively stabilize the film surface, inhibiting ion migration from the surface to the bulk, thus preventing phase segregation. As a result, the carbazole-based WBG PVSC showed a PCE of 20.2%, giving rise to 28.2% efficiency for 2-T perovskite/silicon TSCs.

Yang *et al.* considered positive iodide interstitials as the deep-level defects in the WBG perovskite that greatly limit the PCE of PVSCs.<sup>64</sup> Therefore, they subtly used trimethylphenylammonium tribromide ( $\text{TPABr}_3$ ) as a defect passivator and incorporated  $\text{TPABr}_3$  into the WBG perovskite precursor, inhibiting the formation of iodide interstitials. As proposed in Fig. 5e,  $\text{Br}^-$  occupies the halide sites or fills halide vacancies, leaving two terminal Br atoms. Due to the space limit, the formation of iodide interstitials can be significantly suppressed.

### 4.3 Perovskite surface passivation

Surface passivation is another important engineering strategy aiming at improving the stability of perovskite materials and the device performance.<sup>98</sup> It is a post treatment and adopted to modify the surface of perovskite after its generation.

The perovskite surface is treated with certain organic molecules that can effectively passivate defects.<sup>99,100</sup> These molecules improve the electronic properties of the perovskite surface by reducing trap states and minimizing non-radiative recombination processes. As the deep-level acceptor defects are the major causes of  $V_{\text{oc}}$ , using ammonium salts as anti-solvent to passivate *via* surface gradient passivation (SGP) was proven to be an effective way to passivate defects on the perovskite layer. Yan *et al.* investigated that using a set of molecules sharing the phenylethylamine functional groups but with strategically varying positions of the F atom including PEA (phenylethyl ammonium iodide), and *ortho*-, *meta*-, and *para*-FPEAI (*o/m/p*-FPEAI) through SGP can greatly passivate defects on the  $\text{Cs}_{0.05}(\text{FA}_{0.77}\text{MA}_{0.23})_{0.95}\text{Pb}(\text{I}_{0.77}\text{Br}_{0.23})_3$  perovskite surface as shown in Fig. 6a.<sup>58</sup> Wherein, *p*-FPEAI shows the best passivation performance due to its longer distance between the electron-drawing group (F) and the positively charged terminal ( $-\text{NH}_3^+$ ) which can increase the activity of ammonium ions. The  $\text{PEA}^+$  can effectively passivate  $\text{I}_{\text{Pb}}$  antisite defects and the F atom gives  $\text{PEA}^+$  an excellent ability to passivate  $\text{I}_{\text{A}}$  antisite defects.

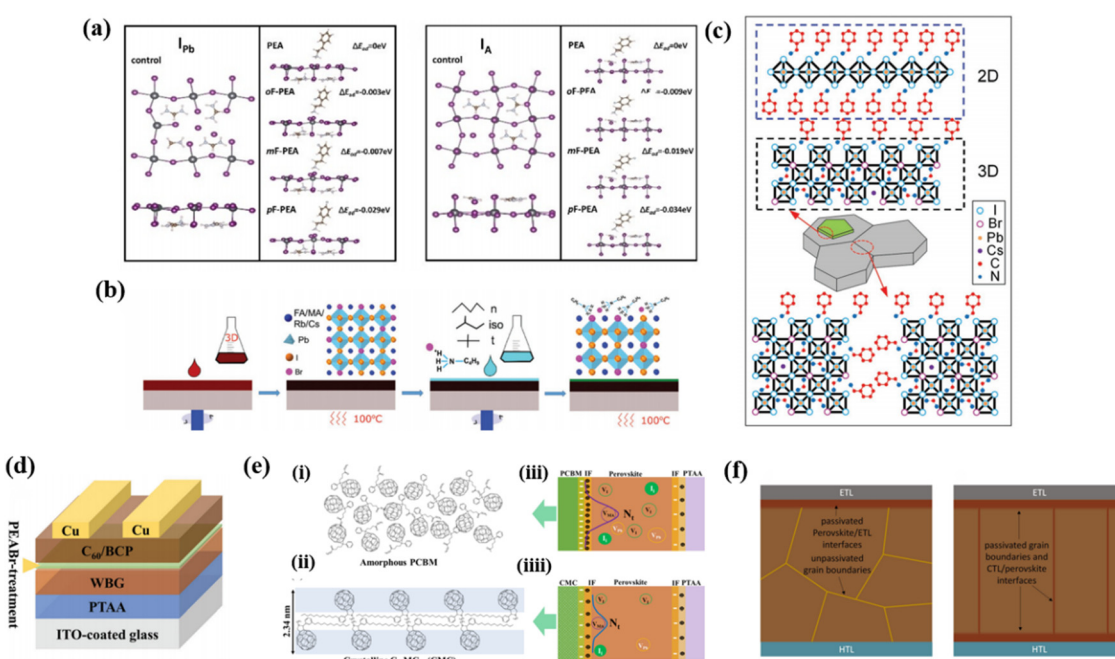


Fig. 6 (a) Schematic diagram of the interaction between ammonium cations and the acceptor-like defects  $\text{I}_{\text{Pb}}$  and  $\text{I}_{\text{A}}$ . Reproduced with permission from ref. 58. Copyright 2023, Wiley-VCH. (b) Schematic detailing the 2D treatment routes for the perovskite solar cell absorber layer by surface coating. Reproduced with permission from ref. 52. Copyright 2020, Wiley-VCH. (c) Schematic of BA modification on the  $\text{Cs}_{0.15}\text{FA}_{0.85}\text{Pb}(\text{I}_{0.73}\text{Br}_{0.27})_3$  thin film. Reproduced with permission from ref. 48. Copyright 2017, Wiley-VCH. (d) Schematic illustration of the device structure with PEABr-treatment. Reproduced with permission from ref. 55. Copyright 2022, Wiley-VCH. (e) Schematic illustration of the mechanism for performance enhancement in device with crystalline fullerene derivatives. Reproduced with permission from ref. 57. Copyright 2018, ACS Appl. (f) Schematic of PEAI and GRBP post treated perovskite films. Reproduced with permission from ref. 50. Copyright 2022, Wiley-VCH.

It is widely used to construct interfacial 2D/3D heterostructures by alkylamines to passivate defects, block ion migration, and suppress phase segregation of PVSCs. After coating different aliphatic alkylammonium bulky cations on the surface of the 3D perovskite, Duong *et al.* identified that a Ruddlesden-Popper quasi-2D perovskite phase can be formed on the surface of the 3D perovskite and effectively passivate surface defects.<sup>52</sup> As shown in Fig. 6b, they took the quadruple-cation mixed-halide perovskite  $\text{Rb}_{0.05}\text{Cs}_{0.095}\text{MA}_{0.1425}\text{FA}_{0.7125}\text{PbI}_2\text{Br}$  with a bandgap of 1.72 eV as the 3D perovskite and firstly spin the 3D perovskite film on a substrate based on a standard procedure, the substrate was subsequently annealed on a hot plate at 100 °C for 30 min. Then the 2D perovskite precursor (*n*-butylammonium bromide (*n*-BABr), iso-BABr, or *t*-BABr dissolved in 2-propanol with different concentrations) was spun on the 3D perovskite film, followed by annealing at 100 °C for 5 min. It is confirmed that the device performance has been greatly enhanced after that as the surface defects have been well modified. Zhou *et al.* introduced benzylamine (BA) post treatment for the 1.72 eV bandgap  $\text{Cs}_{0.15}\text{FA}_{0.85}\text{Pb(I}_{0.73}\text{Br}_{0.27})_3$  perovskite *via* forming a 2D  $\text{BA}_2\text{PbI}_4$  phase as illustrated in Fig. 6c.<sup>48</sup> They have proven that constructing a 2D phase after perovskite formation can effectively passivate defective regions and prevent decomposition or phase segregation. In addition, the formation of 2D  $\text{BA}_2\text{PbI}_4$  produced an energy cascade with the underneath 3D perovskite, which facilitated hole extraction and simultaneously blocked electron transportation. Consequently, the stability and efficiency of the PVSCs were significantly enhanced after BA modification.

Certain chemical treatments can be applied to the perovskite surface to passivate defects and reduce surface energy levels. For example, treatment with Lewis bases or halide salts can lead to the formation of a self-passivating layer on the perovskite surface, thereby improving the device performance and optimizing the surface electric field. As mentioned previously, surface post treatment using ammonium halides can effectively inhibit  $V_{\text{oc}}$  deficit in WBG PVSCs. He *et al.* indicated a phenethylammonium bromide (PEABr) post-treatment strategy to precisely tailor the phase purity of 2D perovskites on the WBG perovskite at different annealing temperatures.<sup>55</sup> As represented in Fig. 6d, after PEABr post-treatment, a pure 2D perovskite phase formed at 60 °C on the top of a 1.77 eV WBG perovskite. Consequently, this self-passivating layer significantly suppressed the defects on the surface, giving the 1.77 eV WBG PVSC a  $V_{\text{oc}}$  of 1.284 V, which is the lowest  $V_{\text{oc}}$  deficit (0.486 V) among WBG PVSCs whose bandgaps were higher than 1.75 eV.

Another method focuses on modifying the interface between the perovskite layer and the CTL. This can be achieved by using suitable interfacial materials that enhance charge extraction and reduce surface recombination. Khadka *et al.* synthesized long alkyl chain-substituted fullerene derivatives as the electron transport layer (ETL).<sup>57</sup> Compared to amorphous  $\text{PC}_{61}\text{BM}$ , the  $\text{C}_{60}$ -fused *N*-methylpyrrolidine-*meta*-dodecyl phenyl ( $\text{C}_{60}\text{MC}_{12}$ ) showed high crystallinity, which contribute to lower perovskite/ETL interfacial defects.<sup>57</sup> The schematic diagrams explained the optimization mechanism. It is supposed that the

surface molecules are randomly oriented in the amorphous PCBM film shown in Fig. 6e(i), while the crystalline CMC film forms well-ordered CMC molecules with a periodic bilayer structure with interlaced dodecyl chains as shown in Fig. 6e(ii). The CMC thin film with a bilayer crystalline structure generates an advantageous perovskite/ETL interface layer, effectively suppressing the traps at the interface. As represented in Fig. 6e(iii), the device with amorphous PCBM builds up more detrimental charges at the PCBM/perovskite interface, causing higher defect densities in the perovskite film. Moreover, the defect distribution may also diffuse into the perovskite layer. In contrast, the defects in the perovskite film of the device with the high crystallinity CMC film were effectively passivated (Fig. 6e(iii)).

In addition, Liu *et al.* proposed a grain regrowth and bifacial passivation (GRBP) strategy to inhibit defects at both grain boundaries and perovskite/CTL interfaces simultaneously as shown in Fig. 6f.<sup>50</sup> A mixture of methylammonium thiocyanate (MASCN) and phenethylammonium iodide (PEAI) was used to conduct a post treatment of perovskite films. The MASN induces the regrowth of perovskite grains and can simultaneously facilitate the penetration of PEAI into the buried interface. Therefore, the bulk and interface non-radiative recombination losses are decreased, and the open circuit voltage of the device is substantially improved. Consequently, PCEs of 21.9% and 19.9% for the 1.65 eV bandgap opaque and semitransparent PVSCs are obtained.

Efficient defect passivation in WBG PVSCs is a vibrant research area. Researchers are continually exploring new materials, surface modification techniques, and interfacial engineering strategies to reduce trap densities, enhance charge carrier lifetimes, and improve the overall stability and efficiency of these devices.

## 5 Conclusion and outlook

Over the past decade, PVSCs have experienced rapid and unparalleled progress. As the bandgap can be easily tuned by composition engineering, the WBG mixed-halide PVSCs have been developed in various PV applications. Among them, the perovskite/Si or perovskite/perovskite tandem solar cells which use WBG PVSCs as the top cells to enhance total efficiency are regarded as one of the most promising PV technologies in the future. However, the WBG PVSCs suffer from large  $V_{\text{oc}}$  deficits and instability issues and the underlying mechanisms are still unknown. Nevertheless, it is undisputed that one of the primary contributors to these issues is the inevitable occurrence of various defects during the perovskite preparation processes. These defects not only act as centers for non-radiative charge carrier recombination and vacancies for ion migration, but also serve as active sites for degradation caused by water and oxygen exposure. Generally, the defects can be classified as positively charged and negatively charged, as the two can be passivated by Lewis bases and Lewis acids, respectively. Furthermore, the defects can be classified by the position of the device, namely the buried-interface defects, the bulk defects, and the surface

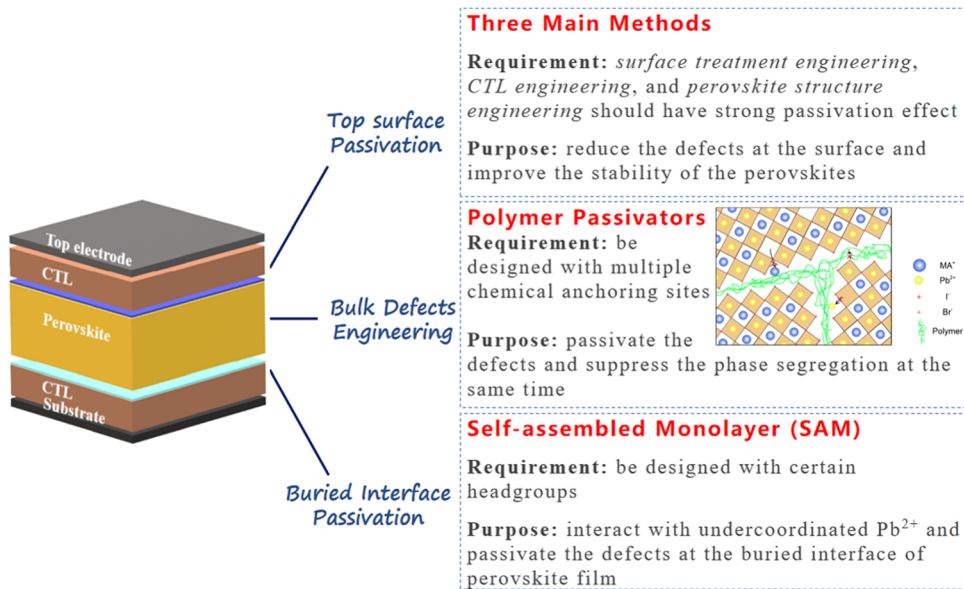


Fig. 7 Some proposed strategies for passivating the defects at the buried interface of perovskite, in perovskite bulk, and at the top of perovskite surface.

defects. To date, massive passivation strategies for these three defects have been introduced and relative devices also exhibited high performances.

For future defect passivation strategies, we provide our perspectives as shown in Fig. 7. For the WBG perovskite buried interface passivation, we believe that using SAMs is one of the most promising methods in the future. Compared to the passivation interlayer engineering between the CTL and the perovskite layer, the SAM molecules can be designed for highly efficient hole or electron extraction, which is beneficial for device performance. On the other hand, the SAM molecules can be designed with certain headgroups, such as ammonium groups ( $-\text{NH}_3^+$ ) and carboxyl ( $-\text{COOH}$ ) groups which can interact with undercoordinated  $\text{Pb}^{2+}$  and thus passivate the defects at the buried interface of the perovskite film. Therefore, material scientists should move forward to design and synthesize novel SAM molecules for perovskites to improve the efficiency and stability of WBG PVSCs in the future.

For the WBG perovskite bulk defects engineering, we recommend using polymer passivators with certain functional groups. As the WBG perovskites tend to exhibit phase segregation under light illumination due to the ion migration and remixing of the halide ions, it is helpful to find materials that not only passivate defects, but also suppress ion migration in the perovskite bulk. Using polymer additives in perovskite precursors shows potential to solve the above-mentioned issue of WBG perovskites. The polymer can be designed with multiple chemical anchoring sites for perovskite defect passivation. On the other hand, polymer additives are generally distributed at the grain boundaries of perovskites. Such network distribution will be a robust shield for ion migration from one grain to another. Therefore, polymer additives have great potential to passivate the defects and suppress phase segregation at the same time. Investigations of the perovskite precursor chemistry

and interaction between perovskite and polymer additives are required to achieve high-efficiency and stable WBG PVSCs.

For defects passivation at the WBG perovskite top surfaces, there are three main methods including surface treatment engineering, CTL engineering, and perovskite structure engineering. For the perovskite surface treatment, novel materials are needed to have a strong passivation effect and at the same time it should be ultrathin to have a negligible effect on the charge transport. For CTL engineering, we believe new polymer-based CTls with certain functional groups are needed to passivate the surface defects. For perovskite structure engineering, forming a thin low-dimensional perovskite layer on the top is a promising strategy to reduce the defects at the surface and improve the stability of the perovskites.

Finally, we believe that upscaling defect passivation engineering is a key step to push the commercialization of PVSCs. The current defect passivators and the passivation methods are not suitable for large-sale device fabrication. New low-cost functional materials as defect passivators are urgently required. Then how to prepare the passivation layer at the buried interface and perovskite top surface on a large-scale is a tricky problem, which requires more contributions from the PV community.

In conclusion, efficient defect passivation in WBG mixed-halide PVSCs remains an active area of research. Many novel materials, surface modification techniques, and interface engineering strategies have been introduced to reduce trap density, improve carrier lifetime, and enhance overall stability and efficiency of the corresponding PV devices. However, there is still a necessity to uncover the nature of the defects in WBG PVSCs. Disclosing the photophysical and chemical properties of the complicated defects is also important to develop novel materials and methods that can passivate the defects. Moreover, strategies to passivate the defects in perovskite bulk and

the interface between the perovskite and the CTLs are still needed to enhance the performance of devices and inhibit phase segregation of the mixed halide perovskites. In addition, developing low-cost passivator materials and exploring defect passivation engineering for upscaling processing is of great importance for future commercialization of WBG mixed-halide PVSCs.

## Conflicts of interest

There are no conflicts to declare.

## References

- 1 S. R. Kellert, Building for life: Designing and understanding the human-nature connection, *Renewable Resour. J.*, 2006, **24**, 8.
- 2 Z. Yue, H. Guo and Y. Cheng, Toxicity of Perovskite Solar Cells, *Energies*, 2023, **16**, 4007.
- 3 A. Alzoubi, Renewable Green hydrogen energy impact on sustainability performance, *Int. J. Comput. Inf. Manuf.*, 2021, **1**, DOI: [10.54489/ijcim.v1i1.46](https://doi.org/10.54489/ijcim.v1i1.46).
- 4 S. Kouro, J. I. Leon, D. Vinnikov and L. G. Franquelo, Grid-connected photovoltaic systems: An overview of recent research and emerging PV converter technology, *IEEE Ind. Electron. Mag.*, 2015, **9**, 47–61.
- 5 A. S. Bati, Y. L. Zhong, P. L. Burn, M. K. Nazeeruddin, P. E. Shaw and M. Batmunkh, Next-generation applications for integrated perovskite solar cells, *Commun. Mater.*, 2023, **4**, 2.
- 6 S.-P. Feng, Y. Cheng, H.-L. Yip, Y. Zhong, P. W. Fong, G. Li, A. Ng, C. Chen, L. A. Castriotta and F. Matteocci, Roadmap on commercialization of metal halide perovskite photovoltaics, *J. Phys. Mater.*, 2023, **6**, 320501.
- 7 Z. Guo, A. K. Jena, G. M. Kim and T. Miyasaka, The high open-circuit voltage of perovskite solar cells: a review, *Energy Environ. Sci.*, 2022, **15**, 3171–3222.
- 8 J. Islam and A. A. Hossain, Semiconducting to metallic transition with outstanding optoelectronic properties of CsSnCl<sub>3</sub> perovskite under pressure, *Sci. Rep.*, 2020, **10**, 14391.
- 9 H. Kim, J. Lim, M. Sohail and M. K. Nazeeruddin, Superhalogen passivation for efficient and stable perovskite solar cells, *Sol. RRL*, 2022, **6**, 2200013.
- 10 Y. Zhou, L. M. Herz, A. K. Jen and M. Saliba, Advances and challenges in understanding the microscopic structure–property–performance relationship in perovskite solar cells, *Nat. Energy*, 2022, **7**, 794–807.
- 11 H. Zhang, L. Xu, B. Han, H. Wang, Y. Liu, P. Wang, P. Lin, X. Wu, X. Yu and C. Cui, PEIE-complexed SnO<sub>2</sub> enabled low-temperature solution fabrication of high-performance CsPbI<sub>3</sub> all-inorganic perovskite solar cells, *J. Alloys Compd.*, 2023, **957**, 170394.
- 12 S. Y. Hong, H. J. Lee, J. K. Park, J. H. Heo and S. H. Im, Acetylacetone modulated TiO<sub>2</sub> nanoparticles for low-temperature solution processable perovskite solar cell, *Int. J. Energy Res.*, 2022, **46**, 22819–22831.
- 13 S. H. Reddy, F. Di Giacomo and A. Di Carlo, Low-temperature-processed stable perovskite solar cells and modules: a comprehensive review, *Adv. Energy Mater.*, 2022, **12**, 2103534.
- 14 L. Lin, T. W. Jones, T. C. J. Yang, N. W. Duffy, J. Li, L. Zhao, B. Chi, X. Wang and G. J. Wilson, Inorganic electron transport materials in perovskite solar cells, *Adv. Funct. Mater.*, 2021, **31**, 2008300.
- 15 Q. Liu, W. Cai, W. Wang, H. Wang, Y. Zhong and K. Zhao, Controlling Phase Transition toward Future Low-Cost and Eco-friendly Printing of Perovskite Solar Cells, *J. Phys. Chem. Lett.*, 2022, **13**, 6503–6513.
- 16 M. R. Samantaray, N. K. Rana, A. Kumar, D. S. Ghosh and N. Chander, Stability study of large-area perovskite solar cells fabricated with copper as low-cost metal contact, *Int. J. Energy Res.*, 2022, **46**, 1250–1262.
- 17 S. Kajal, *Stability enhancement in solution-processed perovskite solar cells*, PhD thesis, Ulsan National Institute of Science and Technology, 2020.
- 18 A. Kojima, K. Teshima, Y. Shirai and T. Miyasaka, Organometal halide perovskites as visible-light sensitizers for photovoltaic cells, *J. Am. Chem. Soc.*, 2009, **131**, 6050–6051.
- 19 P. K. Kung, M. H. Li, P. Y. Lin, Y. H. Chiang, C. R. Chan, T. F. Guo and P. Chen, A review of inorganic hole transport materials for perovskite solar cells, *Adv. Mater. Interfaces*, 2018, **5**, 1800882.
- 20 National Renewable Energy Laboratory (NREL), Best Research-Cell Efficiencies, <https://www.nrel.gov/pv/assets/pdfs/cell-pv-eff-emergingpv.pdf>.
- 21 B. Shi, L. Duan, Y. Zhao, J. Luo and X. Zhang, Semitransparent perovskite solar cells: from materials and devices to applications, *Adv. Mater.*, 2020, **32**, 1806474.
- 22 L. Yang, J. Shi, Y. Wu, X. Jin, T. Bie, C. Hu, W. Liang, Y. Gao, M. Xu and M. Shao, Long Carrier Diffusion Length and Efficient Charge Transport in Thick Quasi-Two-Dimensional Perovskite Solar Cells Enabled by Modulating Crystal Orientation and Phase Distribution, *ACS Appl. Energy Mater.*, 2022, **5**, 8930–8939.
- 23 X. Chu, Q. Ye, Z. Wang, C. Zhang, F. Ma, Z. Qu, Y. Zhao, Z. Yin, H.-X. Deng and X. Zhang, Surface in situ reconstruction of inorganic perovskite films enabling long carrier lifetimes and solar cells with 21% efficiency, *Nat. Energy*, 2023, **8**, 372–380.
- 24 G. O. Odunmbaku, S. Chen, B. Guo, Y. Zhou, N. A. N. Ouedraogo, Y. Zheng, J. Li, M. Li and K. Sun, Recombination pathways in perovskite solar cells, *Adv. Mater. Interfaces*, 2022, **9**, 2102137.
- 25 Y. He, I. Hadar and M. G. Kanatzidis, Detecting ionizing radiation using halide perovskite semiconductors processed through solution and alternative methods, *Nat. Photonics*, 2022, **16**, 14–26.
- 26 H. Hegazy, G. M. Mustafa, A. Nawaz, N. Noor, A. Dahshan and I. Boukhris, Tuning of direct bandgap of Rb<sub>2</sub>ScTlX<sub>6</sub> (X = Cl, Br, I) double perovskites through halide ion

substitution for solar cell devices, *J. Mater. Res. Technol.*, 2022, **19**, 1271–1281.

27 F. Xu, M. Zhang, Z. Li, X. Yang and R. Zhu, Challenges and Perspectives toward Future Wide-Bandgap Mixed-Halide Perovskite Photovoltaics, *Adv. Energy Mater.*, 2023, **13**, 2203911.

28 J. Zheng, G. Wang, W. Duan, M. A. Mahmud, H. Yi, C. Xu, A. Lambertz, S. Bremner, K. Ding and S. Huang, Monolithic perovskite–perovskite–silicon triple-junction tandem solar cell with an efficiency of over 20%, *ACS Energy Lett.*, 2022, **7**, 3003–3005.

29 J. J. Yoo, S. S. Shin and J. Seo, Toward efficient perovskite solar cells: progress, strategies, and perspectives, *ACS Energy Lett.*, 2022, **7**, 2084–2091.

30 C. Liu, H. Dong, Z. Zhang, W. Chai, L. Li, D. Chen, W. Zhu, H. Xi, J. Zhang and C. Zhang, Promising applications of wide bandgap inorganic perovskites in underwater photovoltaic cells, *Sol. Energy*, 2022, **233**, 489–493.

31 A. W. Ho-Baillie, H. G. Sullivan, T. A. Bannerman, H. P. Talathi, J. Bing, S. Tang, A. Xu, D. Bhattacharyya, I. H. Cairns and D. R. McKenzie, Deployment opportunities for space photovoltaics and the prospects for perovskite solar cells, *Adv. Mater. Technol.*, 2022, **7**, 2101059.

32 T. M. Koh, H. Wang, Y. F. Ng, A. Bruno, S. Mhaisalkar and N. Mathews, Halide perovskite solar cells for building integrated photovoltaics: Transforming building façades into power generators, *Adv. Mater.*, 2022, **34**, 2104661.

33 R. Wang, T. Huang, J. Xue, J. Tong, K. Zhu and Y. Yang, Prospects for metal halide perovskite-based tandem solar cells, *Nat. Photonics*, 2021, **15**, 411–425.

34 J. A. Röhr, J. Lipton, J. Kong, S. A. Maclean and A. D. Taylor, Efficiency limits of underwater solar cells, *Joule*, 2020, **4**, 840–849.

35 A. Mahata, D. Meggiolaro and F. De Angelis, From large to small polarons in lead, tin, and mixed lead–tin halide perovskites, *J. Phys. Chem. Lett.*, 2019, **10**, 1790–1798.

36 M. Pratheek, P. Sujith, T. S. Hameed and P. Predeep, Effect of bromide doping on the phase stability and shelf life of the triple cation mixed halide perovskite single-crystals, *Mater. Lett.*, 2022, **326**, 132903.

37 P. Caprioglio, J. A. Smith, R. D. Oliver, A. Dasgupta, S. Choudhary, M. D. Farrar, A. J. Ramadan, Y.-H. Lin, M. G. Christoforo and J. M. Ball, Open-circuit and short-circuit loss management in wide-gap perovskite pin solar cells, *Nat. Commun.*, 2023, **14**, 932.

38 J. Bisquert, Interpretation of the Recombination Lifetime in Halide Perovskite Devices by Correlated Techniques, *J. Phys. Chem. Lett.*, 2022, **13**, 7320–7335.

39 Z. Cui, Q. Zhang, Y. Bai and Q. Chen, Issues of phase segregation in wide-bandgap perovskite, *Mater. Chem. Front.*, 2023, **7**, 1896–1911.

40 A. Hassan, Z. Wang, Y. H. Ahn, M. Azam, A. A. Khan, U. Farooq, M. Zubair and Y. Cao, Recent defect passivation drifts and role of additive engineering in perovskite photovoltaics, *Nano Energy*, 2022, 107579.

41 D. A. Kara, D. Cirak and B. Gultekin, Decreased surface defects and non-radiative recombination via the passivation of the halide perovskite film by 2-thiophenecarboxylic acid in triple-cation perovskite solar cells, *Phys. Chem. Chem. Phys.*, 2022, **24**, 10384–10393.

42 Y. Cheng and L. Ding, Pushing commercialization of perovskite solar cells by improving their intrinsic stability, *Energy Environ. Sci.*, 2021, **14**, 3233–3255.

43 J. Zhao, A. S. Chesman, J. Yan, L. J. Sutherland, J. Jasieniak, J. Lu, W. Mao and U. Bach, Precursor engineering of lead acetate-based precursors for high-open-circuit voltage wide-bandgap perovskite solar cells, *ACS Appl. Mater. Interfaces*, 2023, **15**, 18800–18807.

44 K. Ridzoňová, R. Grill, A. P. Amalathas, B. Dzurňák, N. Neykova, L. Horák, P. Fiala, X. Y. Chin, C. M. Wolff and Q. Jeangros, Correlating light-induced deep defects and phase segregation in mixed-halide perovskites, *J. Mater. Chem. A*, 2022, **10**, 18928–18938.

45 T. Huang, S. Tan, S. Nuryyeva, I. Yavuz, F. Babbe, Y. Zhao, M. Abdelsamie, M. H. Weber, R. Wang and K. N. Houk, Performance-limiting formation dynamics in mixed-halide perovskites, *Sci. Adv.*, 2021, **7**, eabj1799.

46 Y. Bai, Z. Huang, X. Zhang, J. Lu, X. Niu, Z. He, C. Zhu, M. Xiao, Q. Song and X. Wei, Initializing film homogeneity to retard phase segregation for stable perovskite solar cells, *Science*, 2022, **378**, 747–754.

47 J. Liu, E. Aydin, J. Yin, M. De Bastiani, F. H. Isikgor, A. U. Rehman, E. Yengel, E. Uğur, G. T. Harrison and M. Wang, 28.2%-efficient, outdoor-stable perovskite/silicon tandem solar cell, *Joule*, 2021, **5**, 3169–3186.

48 Y. Zhou, F. Wang, Y. Cao, J. P. Wang, H. H. Fang, M. A. Loi, N. Zhao and C. P. Wong, Benzylamine-treated wide-bandgap perovskite with high thermal-photostability and photovoltaic performance, *Adv. Energy Mater.*, 2017, **7**, 1701048.

49 Y. Zhou, Y. H. Jia, H. H. Fang, M. A. Loi, F. Y. Xie, L. Gong, M. C. Qin, X. H. Lu, C. P. Wong and N. Zhao, Composition-tuned wide bandgap perovskites: From grain engineering to stability and performance improvement, *Adv. Funct. Mater.*, 2018, **28**, 1803130.

50 Z. Liu, C. Zhu, H. Luo, W. Kong, X. Luo, J. Wu, C. Ding, Y. Chen, Y. Wang and J. Wen, Grain Regrowth and Bifacial Passivation for High-Efficiency Wide-Bandgap Perovskite Solar Cells, *Adv. Energy Mater.*, 2023, **13**, 2203230.

51 H. Xu, Z. Liang, J. Ye, S. Xu, Z. Wang, L. Zhu, X. Chen, Z. Xiao, X. Pan and G. Liu, Guanidinium-assisted crystallization modulation and reduction of open-circuit voltage deficit for efficient planar  $\text{FAPbBr}_3$  perovskite solar cells, *Chem. Eng. J.*, 2022, **437**, 135181.

52 T. Duong, H. Pham, T. C. Kho, P. Phang, K. C. Fong, D. Yan, Y. Yin, J. Peng, M. A. Mahmud and S. Gharibzadeh, High efficiency perovskite–silicon tandem solar cells: effect of surface coating versus bulk incorporation of 2D perovskite, *Adv. Energy Mater.*, 2020, **10**, 1903553.

53 D. Wang, H. Guo, X. Wu, X. Deng, F. Li, Z. Li, F. Lin, Z. Zhu, Y. Zhang and B. Xu, Interfacial engineering of wide-bandgap perovskites for efficient perovskite/CZTSSe tandem solar cells, *Adv. Funct. Mater.*, 2022, **32**, 2107359.

54 M. Abdi-Jalebi, Z. Andaji-Garmaroudi, S. Cacovich, C. Stavrakas, B. Philippe, J. M. Richter, M. Alsari, E. P. Booker, E. M. Hutter and A. J. Pearson, Maximizing and stabilizing luminescence from halide perovskites with potassium passivation, *Nature*, 2018, **555**, 497–501.

55 R. He, Z. Yi, Y. Luo, J. Luo, Q. Wei, H. Lai, H. Huang, B. Zou, G. Cui and W. Wang, Pure 2D Perovskite Formation by Interfacial Engineering Yields a High Open-Circuit Voltage beyond 1.28 V for 1.77 eV Wide-Bandgap Perovskite Solar Cells, *Adv. Sci.*, 2022, **9**, 2203210.

56 X. Huo, Y. Li, Y. Lu, J. Dong, Y. Zhang, S. Zhao, B. Qiao, D. Wei, D. Song and Z. Xu, Suppressed halide segregation and defects in wide bandgap perovskite solar cells enabled by doping organic bromide salt with moderate chain length, *J. Phys. Chem. C*, 2022, **126**, 1711–1720.

57 D. B. Khadka, Y. Shirai, M. Yanagida, T. Noda and K. Miyano, Tailoring the open-circuit voltage deficit of wide-band-gap perovskite solar cells using alkyl chain-substituted fullerene derivatives, *ACS Appl. Mater. Interfaces*, 2018, **10**, 22074–22082.

58 N. Yan, Y. Gao, J. Yang, Z. Fang, J. Feng, X. Wu, T. Chen and S. Liu, Wide-Bandgap Perovskite Solar Cell Using a Fluoride-Assisted Surface Gradient Passivation Strategy, *Angew. Chem., Int. Ed.*, 2023, **62**, e202216668.

59 L. Wang, W. Zheng, F. Vitale, X. Zhang, X. Li, Y. Ji, Z. Liu, O. Ghaebi, C. T. Plass and R. Domes, Wide-Bandgap Double Perovskites with Multiple Longitudinal-Optical Phonon Scattering, *Adv. Funct. Mater.*, 2022, **32**, 2111338.

60 H. Jiao, Z. Ni, Z. Shi, C. Fei, Y. Liu, X. Dai and J. Huang, Perovskite grain wrapping by converting interfaces and grain boundaries into robust and water-insoluble low-dimensional perovskites, *Sci. Adv.*, 2022, **8**, eabq4524.

61 W. Wang, M. Cai, Y. Wu, K. Ji, B. Cheng, X. Liu, H. Lv and S. Dai, Defect healing of MAPbI<sub>3</sub> perovskite single crystal surface by benzylamine, *Symmetry*, 2022, **14**, 1099.

62 Z. Li, X. Zheng, X. Xiao, Y. An, Y. Wang, Q. Huang, X. Li, R. Cheacharoen, Q. An and Y. Rong, Beyond the Phase Segregation: Probing the Irreversible Phase Reconstruction of Mixed-Halide Perovskites, *Adv. Sci.*, 2022, **9**, 2103948.

63 L. A. Muscarella and B. Ehrler, The influence of strain on phase stability in mixed-halide perovskites, *Joule*, 2022, **6**, 2016–2031.

64 G. Yang, Z. Ni, Z. J. Yu, B. W. Larson, Z. Yu, B. Chen, A. Alasfour, X. Xiao, J. M. Luther and Z. C. Holman, Defect engineering in wide-bandgap perovskites for efficient perovskite–silicon tandem solar cells, *Nat. Photonics*, 2022, **16**, 588–594.

65 G. K. Grandhi, D. Hardy, M. Krishnaiah, B. Vargas, B. Al-Anesi, M. P. Suryawanshi, D. Solis-Ibarra, F. Gao, R. L. Hoye and P. Vivo, Wide-Bandgap Perovskite-Inspired Materials: Defect-Driven Challenges for High-Performance Optoelectronics, *Adv. Funct. Mater.*, 2023, 2307441.

66 Y. Yu, R. Liu, F. Zhang, C. Liu, Q. Wu, M. Zhang and H. Yu, Potassium tetrafluoroborate-induced defect tolerance enables efficient wide-bandgap perovskite solar cells, *J. Colloid Interface Sci.*, 2022, **605**, 710–717.

67 H. Xue, G. Brocks and S. Tao, Intrinsic defects in primary halide perovskites: A first-principles study of the thermodynamic trends, *Phys. Rev. Mater.*, 2022, **6**, 055402.

68 T. Nie, J. Yang, Z. Fang, Z. Xu, X. Ren, X. Guo, T. Chen and S. F. Liu, Amino-acid-type alkylamine additive for high-performance wide-bandgap perovskite solar cells, *Chem. Eng. J.*, 2023, **468**, 143341.

69 Y. Cheng, X. Liu, Z. Guan, M. Li, Z. Zeng, H. W. Li, S. W. Tsang, A. G. Aberle and F. Lin, Revealing the degradation and self-healing mechanisms in perovskite solar cells by sub-bandgap external quantum efficiency spectroscopy, *Adv. Mater.*, 2021, **33**, 2006170.

70 J. Kim, C.-H. Chung and K.-H. Hong, Understanding of the formation of shallow level defects from the intrinsic defects of lead tri-halide perovskites, *Phys. Chem. Chem. Phys.*, 2016, **18**, 27143–27147.

71 J. Liu, M. Wang, J. Lin, G. Chen, B. Liu, J. Huang, M. Zhang, G. Liang, L. Lu and P. Xu, Mitigating deep-level defects through a self-healing process for highly efficient wide-bandgap inorganic CsPbI<sub>3-x</sub>Br<sub>x</sub> perovskite photovoltaics, *J. Mater. Chem. A*, 2022, **10**, 17237–17245.

72 T. Nie, Z. Fang, X. Ren, Y. Duan and S. Liu, Recent Advances in Wide-Bandgap Organic–Inorganic Halide Perovskite Solar Cells and Tandem Application, *Nano-Micro Lett.*, 2023, **15**, 70.

73 T. Wang, Y. Li, Q. Cao, J. Yang, B. Yang, X. Pu, Y. Zhang, J. Zhao, Y. Zhang and H. Chen, Deep defect passivation and shallow vacancy repair via an ionic silicone polymer toward highly stable inverted perovskite solar cells, *Energy Environ. Sci.*, 2022, **15**, 4414–4424.

74 Z. Ni, H. Jiao, C. Fei, H. Gu, S. Xu, Z. Yu, G. Yang, Y. Deng, Q. Jiang and Y. Liu, Evolution of defects during the degradation of metal halide perovskite solar cells under reverse bias and illumination, *Nat. Energy*, 2022, **7**, 65–73.

75 Y. Cai, J. Cui, M. Chen, M. Zhang, Y. Han, F. Qian, H. Zhao, S. Yang, Z. Yang and H. Bian, Multifunctional enhancement for highly stable and efficient perovskite solar cells, *Adv. Funct. Mater.*, 2021, **31**, 2005776.

76 C. Xu, Z. Zhang, S. Zhang, H. Si, S. Ma, W. Fan, Z. Xiong, Q. Liao, A. Sattar and Z. Kang, Manipulation of perovskite crystallization kinetics via Lewis base additives, *Adv. Funct. Mater.*, 2021, **31**, 2009425.

77 J. Jeong, M. Kim, J. Seo, H. Lu, P. Ahlawat, A. Mishra, Y. Yang, M. A. Hope, F. T. Eickemeyer and M. Kim, Pseudo-halide anion engineering for  $\alpha$ -FAPbI<sub>3</sub> perovskite solar cells, *Nature*, 2021, **592**, 381–385.

78 Y. Qi, K. A. Green, G. Ma, S. Jha, K. Gollinger, C. Wang, X. Gu, D. Patton, S. E. Morgan and Q. Dai, Passivation of iodine vacancies of perovskite films by reducing iodine to triiodide anions for high-performance photovoltaics, *Chem. Eng. J.*, 2022, **438**, 135647.

79 Y. Niu, D. He, X. Zhang, L. Hu and Y. Huang, Enhanced Perovskite Solar Cell Stability and Efficiency via Multi-Functional Quaternary Ammonium Bromide Passivation, *Adv. Mater. Interfaces*, 2023, **10**, 2201497.

80 X. Gong, L. Guan, H. Pan, Q. Sun, X. Zhao, H. Li, H. Pan, Y. Shen, Y. Shao and L. Sun, Highly efficient perovskite solar cells via nickel passivation, *Adv. Funct. Mater.*, 2018, **28**, 1804286.

81 L. Liu, Y. Yang, M. Du, Y. Cao, X. Ren, L. Zhang, H. Wang, S. Zhao, K. Wang and S. Liu, Self-Assembled Amphiphilic Monolayer for Efficient and Stable Wide-Bandgap Perovskite Solar Cells, *Adv. Energy Mater.*, 2023, **13**, 2202802.

82 Z. Xing, S.-H. Li and S. Yang, Targeted Molecular Design of Functionalized Fullerenes for High-Performance and Stable Perovskite Solar Cells, *Small Struct.*, 2022, **3**, 2200012.

83 Z. Fang, L. Jia, N. Yan, X. Jiang, X. Ren, S. Yang and S. Liu, Proton-transfer-induced *in situ* defect passivation for highly efficient wide-bandgap inverted perovskite solar cells, *InfoMat*, 2022, **4**, e12307.

84 L. Yang, Y. Jin, Z. Fang, J. Zhang, Z. Nan, L. Zheng, H. Zhuang, Q. Zeng, K. Liu and B. Deng, Efficient Semi-Transparent Wide-Bandgap Perovskite Solar Cells Enabled by Pure-Chloride 2D-Perovskite Passivation, *Nano-Micro Lett.*, 2023, **15**, 111.

85 M. Jaysankar, B. A. Raul, J. Bastos, C. Burgess, C. Weijtens, M. Creatore, T. Aernouts, Y. Kuang, R. Gehlhaar and A. Hadipour, Minimizing voltage loss in wide-bandgap perovskites for tandem solar cells, *ACS Energy Lett.*, 2018, **4**, 259–264.

86 F. Ali, C. Roldán-Carmona, M. Sohail and M. K. Nazeeruddin, Applications of self-assembled monolayers for perovskite solar cells interface engineering to address efficiency and stability, *Adv. Energy Mater.*, 2020, **10**, 2002989.

87 J. Zeng, L. Bi, Y. Cheng, B. Xu and A. K.-Y. Jen, Self-assembled monolayer enabling improved buried interfaces in blade-coated perovskite solar cells for high efficiency and stability, *Nano Res. Energy*, 2022, **1**, e9120004.

88 K. Choi, H. Choi, J. Min, T. Kim, D. Kim, S. Y. Son, G.-W. Kim, J. Choi and T. Park, A short review on interface engineering of perovskite solar cells: a self-assembled monolayer and its roles, *Sol. RRL*, 2020, **4**, 1900251.

89 A. Al-Ashouri, A. Magomedov, M. Roß, M. Jošt, M. Talaikis, G. Chistiakova, T. Bertram, J. A. Márquez, E. Köhnen and E. Kasparavičius, Conformal monolayer contacts with lossless interfaces for perovskite single junction and monolithic tandem solar cells, *Energy Environ. Sci.*, 2019, **12**, 3356–3369.

90 Y. Hou, X. Du, S. Scheiner, D. P. McMeekin, Z. Wang, N. Li, M. S. Killian, H. Chen, M. Richter and I. Levchuk, A generic interface to reduce the efficiency-stability-cost gap of perovskite solar cells, *Science*, 2017, **358**, 1192–1197.

91 Y. Yao, C. Cheng, C. Zhang, H. Hu, K. Wang and S. De Wolf, Organic hole-transport layers for efficient, stable, and scalable inverted perovskite solar cells, *Adv. Mater.*, 2022, **34**, 2203794.

92 I. M. Hermes, Y. Hou, V. W. Bergmann, C. J. Brabec and S. A. Weber, The interplay of contact layers: How the electron transport layer influences interfacial recombination and hole extraction in perovskite solar cells, *J. Phys. Chem. Lett.*, 2018, **9**, 6249–6256.

93 L. Zhou, M. Yan, G. Luo, L. Xu, Y. Fang and D. Yang, Self-Assembled Molecule Doping Enables High-Efficiency Hole-Transport-Layer-Free Perovskite Light-Emitting Diodes, *Adv. Funct. Mater.*, 2023, 2303370.

94 Z. Chu, X. Chu, Y. Zhao, Q. Ye, J. Jiang, X. Zhang and J. You, Emerging low-dimensional crystal structure of metal halide perovskite optoelectronic materials and devices, *Small Struct.*, 2021, **2**, 2000133.

95 F. Meng, X. Shang, D. Gao, W. Zhang and C. Chen, Functionalizing phenethylammonium by methoxy to achieve low-dimensional interface defects passivation for efficient and stable perovskite solar cells, *Nanotechnology*, 2021, **33**, 065201.

96 J. Zhu, Y. Qian, Z. Li, O. Y. Gong, Z. An, Q. Liu, J. H. Choi, H. Guo, P. J. Yoo and D. H. Kim, Defect Healing in FAPb(I<sub>1-x</sub>Br<sub>x</sub>)<sub>3</sub> Perovskites: Multifunctional Fluorinated Sulfonate Surfactant Anchoring Enables > 21% Modules with Improved Operation Stability, *Adv. Energy Mater.*, 2022, **12**, 2200632.

97 H. Tan, F. Che, M. Wei, Y. Zhao, M. I. Saidaminov, P. Todorović, D. Broberg, G. Walters, F. Tan and T. Zhuang, Dipolar cations confer defect tolerance in wide-bandgap metal halide perovskites, *Nat. Commun.*, 2018, **9**, 3100.

98 M. A. R. Laskar, W. Luo, N. Ghimire, A. H. Chowdhury, B. Bahrami, A. Gurung, K. M. Reza, R. Pathak, R. S. Bobba and B. S. Lamsal, Phenylhydrazinium iodide for surface passivation and defects suppression in perovskite solar cells, *Adv. Funct. Mater.*, 2020, **30**, 2000778.

99 J. Li, F. Gao, J. Wen, Z. Xu, C. Zhang, X. Hua, X. Cai, Y. Li, B. Shi and Y. Han, Effective surface passivation with 4-bromo-benzonitrile to enhance the performance of perovskite solar cells, *J. Mater. Chem. C*, 2021, **9**, 17089–17098.

100 J. Li, T. Bu, Z. Lin, Y. Mo, N. Chai, X. Gao, M. Ji, X.-L. Zhang, Y.-B. Cheng and F. Huang, Efficient and stable perovskite solar cells via surface passivation of an ultrathin hydrophobic organic molecular layer, *Chem. Eng. J.*, 2021, **405**, 126712.